Luckett, Richard; **Baptie, Brian**. 2015 Local earthquake tomography of Scotland. *Geophysical Journal International*, 200 (3). 1538-1554. 10.1093/gji/ggu489

Local Earthquake Tomography of Scotland

Richard Luckett and Brian Baptie

Keywords: seismic tomography

Abstract

Scotland is a relatively aseismic region for the use of local earthquake tomography, but 40 years of earthquakes recorded by a good and growing network make it possible. A careful selection is made from the earthquakes located by the British Geological Survey (BGS) over the last four decades to provide a dataset maximising arrival time accuracy and ray-path coverage of Scotland. A large number of 1-D velocity models with different layer geometries are considered and differentiated by employing quarry blasts as ground-truth events. Then, SIMULPS14 is used to produce a robust 3-D tomographic P-wave velocity model for Scotland. In areas of high resolution the model shows good agreement with previously published interpretations of seismic refraction and reflection experiments. However, the model shows relatively little lateral variation in seismic velocity except at shallow depths, where sedimentary basins such as the Midland Valley are apparent. At greater depths, higher velocities in the northwest parts of the model suggest that the thickness of crust increases towards the south and east. This observation is also in agreement with previous studies. Quarry blasts used as ground truth events and relocated with the preferred 3-D model are shown to be markedly more accurate than when located with the existing BGS 1-D velocity model.

Introduction

Much of our understanding of seismic velocities in the Earth's crust under the British Isles comes from active source seismic refraction and reflection experiments. However, most of these studies have been offshore, where a dense array of seismic profiles has been gathered by BIRPS (British Institutions Reflection Profiling Syndicate) (Klemperer and Hobbs, 1992). Onshore, crustal structure is constrained by a much smaller number of profiles: LISPB, a north-south profile through Scotland and northern England (Bamford *et al.*, 1978, Barton, 1992); LISPB-Delta, a profile from the north coast of Wales to the English Channel (Edwards and Blundell, 1984, Maguire *et al.*, 2011); CSSP, an east-west profile along the Iapetus Suture line (Bott *et al.*, 1985); and, ICSSP, an extension of CSSP into Ireland (Jacob *et al.*, 1985). (Kelly *et al.*, 2007) attempted to combine data from a number of controlled source experiments, both onshore and offshore, to produce a 3-D seismic velocity model for the crust under the UK and surrounding area but found that velocities were poorly constrained for areas away from the original input data. The onshore experiments have been re-interpreted a number of times, but there is general agreement that the crust primarily consists of three main layers of variable thickness. In addition, the results have been used to construct a number of 1-D seismic velocity models that have been routinely used to locate earthquakes that occur in various parts of the British Isles (Booth *et al.*, 2001). Although there are relatively strong variations in the spatial distribution of seismicity across the British Isles, the diffuse nature of earthquake locations means that it is difficult to accurately map earthquakes to specific faults. The relationship between earthquakes and underlying geology remains unclear, with a number of possible explanations (e.g. Bott and Bott, 2004, Arrowsmith *et al.*, 2005, Main *et al.*, 1999).

In the last ten years, the subsurface of the British Isles has also been investigated using passive seismic methods. (Arrowsmith *et al.*, 2005) used teleseismic body wave tomography to identify a low velocity anomaly in the upper mantle beneath the British Isles. (Hardwick, 2008) constructed 3-D seismic velocity models for England and Wales using local earthquake tomography that broadly agree with observed geology. (Asencio *et al.*, 2003), (Tomlinson, 2006), (Di Leo *et al.*, 2009) and (Davis *et al.*, 2012) all use teleseismic receiver functions to identify various features of the crust and upper mantle under the UK, including the thickness of the crust. However, to date, there have been no published studies that have used local earthquake tomography to image the crust under the northern part of the British Isles.

Local earthquake tomography (Kissling, 1988) is a passive method to image the seismic velocity of the crust. Unlike teleseismic tomography (Aki *et al.*, 1977), it depends on earthquake sources within the model volume. This means that it is generally reserved for seismically active areas. Even in such areas, a uniform distribution of sources and stations is important, as otherwise the model is variably sampled and artefacts can be introduced into the solution. In local earthquake tomography the volume of investigation needs to be adequately sampled by a dense set of crossing rays (a function of the source-receiver distribution) to resolve the inherent trade-off between variations in velocity structure and hypocentre locations. As the data are generally only sampled at relatively few points on the Earth's surface they are typically aliased spatially and the resolution of the image is therefore limited by the distribution of rays (both in the ray path location and its direction) within the target volume (Evans *et al.*, 1994).

Although earthquake activity in Scotland is low, over thirty years of continuous seismic monitoring with a relatively high station density, along with a number of other temporary deployments of instrumentation, means that there are now a sufficient number of recorded earthquakes within the proposed source volume for local earthquake tomography to be used to determine 3-D models of seismic velocity under Scotland and to use these models to relocate the earthquakes in the catalogue.

In this study the seismic velocity structure under Scotland is inverted for simultaneously with the locations of the earthquakes used. This is done using computer algorithm SIMULPS developed by Thurber (Thurber, 1983), which is a damped least squares, full matrix inversion method. The times of first P-wave arrivals from 405 of the best located local earthquakes are used to solve for a number of 3-D velocity models. Quarry blasts from the database are used as ground truth events to evaluate these models and select the final solution. The new earthquake locations found with the new velocity model are considered and the model compared with previous work on the velocity structure in Scotland.

Geology

The surface geology of Scotland (Figure 1) can be split, at the most simplistic level, into three bands running from southwest to northeast. The Highlands are composed of Precambrian metamorphic rocks folded and faulted during the Caledonian and Grampian orogenies. The Midland Valley is a late Devonian graben filled with upper Palaeozoic sediments. The Southern Uplands are an accretionary wedge formed by the closure of the Iapetus Ocean and are composed largely of weakly metamorphosed greywacke.

At a slightly more detailed level, the Highlands are made up of 3 terranes, the Hebridean Terrane, the Northern Highlands and the Grampians. The Hebridean Terrane is northwest of the Moine Thrust and consists of Archaean and Paleoproterozoic granitic to tonalitic gneisses of the Lewisian complex, overlain to the east by Neoprotozoic Torridonian sandstones. The Northern Highlands is the area east of the Moine Thrust and north of the Great Glen Fault. The mountains here are largely made up of Neoproterozoic Moine Supergroup metasedimentary rocks, thought to have been thrust over a basement of Lewisian rocks in the Silurian (Coward, 1983). Gneiss inliers outcrop throughout the Northern Highlands and have been shown (Woodcock and Strachan, 2000) to be similar to Lewisian gneisses. The Grampians Highlands to the SE of the Great Glen Fault are composed of rocks of the Dalradian Supergroup aged between the late Precambrian and the Ordovician. These are metamorphosed sedimentary strata, now tightly folded and mainly found in the form of schists, schistose grit, greywacke and conglomerate. Granite intrusions also occur widely. Based on the velocity model in (Barton, 1992) and observations from the BIRPS offshore reflection data (Klemperer and Hobbs, 1992), it is probable that the Northern Highlands and the Grampians are underlain by physically similar basement rocks. In addition, there is a band of Paleogene volcanic rocks along the West coast of the Highlands from Skye to Arran related to the opening of the Atlantic Ocean and extensive uplift resulting from the underlying mantle plume. Basaltic rocks are most common and are best observed in the Inner Hebridean islands of Mull and Skye where basaltic lavas are up to 2 km thick. Offshore, to the northwest, basaltic lavas thicken, reaching thicknesses of up to 5 km on the Faroe Islands.

Separated from the Grampian Highlands by the Highland Boundary Fault is the Midland Valley. Paleozoic sediments overlie a concealed complex Neoprotozoic metamorphic basement interpreted as a magmatic arc and proximal fore-arc region located on the southern margin of Laurentia (Strachan, 2000). There are numerous Carboniferous igneous intrusions, often apparent at the surface as volcanic edifices. To the south, the Southern Uplands Fault marks the start of the Southern Uplands, which are comprised of Ordovician and Silurian rocks that were once sands and muds deposited on the floor of the Iapetus Ocean. The Ballantrae Complex outcrops along the West coast of the Southern Uplands but is also exposed on higher ground inland. It has been interpreted as an ophiolite complex and may extend to perhaps 40 – 50km in depth (Stone and Smellie, 1988).

Data

In 1969, the predecessor of the British Geological Survey (BGS), the Institute of Geological Sciences, installed the first modern seismometers in Britain, a network of eight seismometers across the lowlands of Scotland. Since then, these stations have remained running and other networks have been added by the BGS across the UK in response to seismic activity or commercial interest. In Scotland, these include networks installed in 1979 on Shetland and based around the Kyle of Lochalsh, a network around the Moray Firth installed in 1981 and a network based at Eskdalemuir in Dumfries and Galloway installed in 1983. Networks were installed at Paisley in 1985, Galloway in 1990, the Borders in 1992 and in Orkney and around the Minch in 1995. The complete network is shown in Figure 2 with BGS stations marked in red.

Data acquisition for each sub-network consisted of a triggered recording system and routine analysis of the resulting waveforms included manual picking and association of phases, discrimination of event types and determination of locations and magnitudes of the resulting seismic events. Origin,

phase and waveform data for all seismic events were archived in a database of instrumentally recorded seismic activity that extends from 1969 to present. This has resulted in a catalogue of 2005 earthquakes between latitudes of 54° and 59.5° and longitudes of -8° and -1.5°. The location of the sub-networks within the UK means that detection capability is not uniform, with smaller earthquakes located in the vicinity of the sub-networks than elsewhere. However, the catalogue is complete from 1979 onwards for all onshore earthquakes with magnitudes of 2.5 or greater (Simpson, 2007). These 2005 events were manually reanalysed to assess the quality of the phase data. Finally, only those earthquakes relocated with a minimum of six P-phases and an azimuthal gap of less than 270° were used in the tomography. If an azimuthal gap of 180° instead of 270° were chosen then 102 more events would be excluded, making the dataset too small.

In addition to the data from BGS stations, data were used from the Reflections Under the Scottish Highlands (RUSH II) passive seismic experiment (Bastow *et al.*, 2007). This experiment consisted of 21 broadband sensors deployed in a north-south line across northwest Scotland between 2001 and 2003 (blue symbols on Figure 2), for which continuous data was available. Data from these stations were used to increase the number of phases for previously detected events in the time period of operation. A detection algorithm applied to the continuous data resulted in the detection of a number of additional earthquakes that had previously gone undetected, ten of which met the selection criteria given above. In total, 405 earthquakes were used for this study with 5890 P-phase picks and 2482 S-phase picks. Uncertainties in arrival times were assumed to average 0.03 seconds. Phases were almost all fully weighted and distance based weights were not used. Phases that were difficult to pick were generally not included. Only 37 phases were downweighted, mostly to 50%. The events and the ray paths contributed to the tomography by each event are shown on Figure 3.

Minimum 1-D velocity model

The 3-D velocity model output by local earthquake tomography has been shown to depend strongly on the initial reference model used (Kissling *et al.*, 1994). As in many previous studies ((Kissling *et al.*, 1995), etc) the computer program VELEST (Kissling, 1995) was used to invert simultaneously for the earthquake locations, station corrections and 1-D velocity model needed as input for the tomography. About 2400 VELEST runs were carried out to achieve the best 1-D model possible. Since there were insufficient good-quality S-wave arrivals to solve separately for a P-wave velocity model and an S-wave velocity model, observed S-wave arrivals were included in the inversion by assuming a fixed *Vp/Vs* ratio. The ratio used was found by making a compound Wadati plot of the entire data set. The value found was 1.72 with a standard deviation of 0.03, which falls within the ranges found using receiver functions by (Di Leo *et al.*, 2009) and (Tomlinson, 2006) and is close to the 1.74 value found by (Davis *et al.*, 2012). Station corrections were calculated relative to station ELO (Figure 2), a station in the centre of Scotland that was used in over half of the events. VELEST does not adjust model layer thickness as part of the inversion, only the velocities in each layer. Four initial combinations of layer boundaries were used:

1) The six layer boundaries from the BGS velocity model for Scotland, which is derived from the LISPB active source experiment (Bamford *et al.*, 1976). The seed velocities were those from the BGS model.

2) The same as 1) but with additional boundaries between those in the BGS model, making a 16 layer model. The seed velocities were those from the BGS model – i.e. neighbouring layers had the same velocity if within the same layer of the original model.

3) and 4) Two different sets of 16 equally spaced layers. Preliminary velocities for each layer were found by increasing the velocity for each layer slightly as depth increased.

For each set of layers, 300 starting velocity models were generated by perturbing the preliminary velocities by up to ±1.5 kms^{-1} with no velocity inversions allowed. The resulting 1200 models were then used as initial conditions for VELEST, along with the selected hypocentres. It was found that nine iterations of VELEST usually did not result in a stable model (that is one which would not change if a 10^{th} iteration was carried out). To rectify this each run of VELEST was followed by a second run of nine iterations, starting with the model and station corrections output by the first run but returning to the original hypocentres. This was found to result in stable models with lower residuals than a single run. After each inversion was complete the resulting model was simplified by velocity layers with the same velocity (within 0.02 kms^{-1}) being combined. This resulted in models with between five and ten layers.

The 1200 resulting models (figure 4) were then evaluated along with their associated hypocentres and station corrections. The average root-mean-squared (rms) residual for the locations with each model is perhaps the most obvious criteria but it was found that a variety of different models produced very similar residuals (of the 1200 models generated 142 had an rms within 5% of the lowest model, 0.20). Two tests were carried out to decide which of these 142 models was the best. The thresholds imposed for these tests were adjusted to make passing the test more difficult until a manageable number of models passed.

For the first test, 54 blasts from eleven quarries were located with each model and station correction set. These blasts were chosen because of evidence showing exactly where they originated and to give as wide a geographical spread as possible (Figure 5 shows the location of the quarries and the spread of stations contributing to these events). In the case of the largest quarries, such as Glensanda many blasts were included at various times as the blasts were recorded by different stations in different years. The locations were done with VELEST, set to do 5 iterations solving only for hypocentres. The starting locations for the blasts were those in the BGS database, which were located in the normal way. The results were compared with the true quarry locations and models were discarded that, on average, mislocated the quarries by more than 5 km or resulted in solutions with an average depth greater than 500 m. These were reasonable but arbitrary thresholds that reduced the number of models to a desired degree. The values used reduced the number of possible 1-D minimum velocity models being considered from 142 to 23.

For the second test, the original hypocentres were randomly perturbed in latitude and longitude by up to 0.1 degree and in depth by up to 5 km. These shifted events were then relocated using each model. The resulting locations were compared to the final locations found in combination with that model during the joint inversion. This is a measure of how shallow the minimum associated with that model is. Any model that, when used for location, produced hypocentres more than 500 m away from the previous locations associated with that model was discarded. This resulted in nine models being considered at the next stage. As can be seen in Figure 6, these models are essentially very similar to each other, despite having different numbers of layers. Station corrections were also very similar for the nine models. Figure 7 shows the station corrections corresponding to Model 2,

which is the model used. It should be noted that model 2 is the model with the highest velocity in the top layer. This layer is poorly constrained, with few ray paths, and will couple strongly with the station corrections. Husen *et al.*, (2003) state that "station delays are only meaningful if more than 10 observations per station exist", such corrections are marked in white in the figure and are not interpreted. Otherwise, the corrections seem reasonable with positive corrections in the Midland Valley and around the Solway Firth/Vale of Eden, indicating that the near surface seismic velocity close to these stations is lower than average for that part of the model. Station corrections are also positive on the west coast of the Scotland around Skye. These station corrections remained largely unchanged throughout the local earthquake tomography that follows because station corrections were heavily damped.

Out of interest, the 1610 reanalysed earthquakes which were not used in velest were relocated with the chosen minumum-1D model, including station corrections. The resulting hypocentres had a slightly lower average residual (by 0.05 seconds) and had moved, on average about 2 km. The new hypocentres were consistently deeper, with depths on average 1 km greater.

Local Earthquake Tomography

We apply the inversion method and computer algorithm SIMULPS developed by (Thurber, 1983) and (Eberhart-Phillips, 1990) (documentation provided by Evans *et al.*, 1994). SIMULPS is a damped least squares, full matrix inversion method intended for use with natural local earthquakes and controlled sources. P arrival times and S minus P times can be inverted to get a velocity model, earthquake locations and station corrections. The algorithm uses a combination of parameter separation (Pavlis and Booker, 1980), (Spencer and Gubbins, 1980) and damped least squares inversion to solve for the model perturbations. The resolution and covariance matrix is computed in order to estimate the resolution of the model and the uncertainties in the model parameters.

The tomography here was carried out using SIMULPS14, a version of SIMULPS incorporating full 3-D ray shooting (Haslinger and Kissling, 2001). Arrival times and earthquake locations are used to invert for velocity at the intersections of a 3-dimensional grid (velocities between these points are interpolated for). Once a new model has been obtained the hypocentres are relocated and variances calculated to check that the model is improving. For the least-squares inversion, damping is applied to the diagonal elements of the matrix to avoid singular values and spurious model changes. The value of damping used can heavily influence results and resolution (Kissling *et al.*, 2001). For this study an optimum damping value of 300 was determined using a trade-off curve between data variance and model variance obtained by a series of single iteration inversions for different damping values (Eberhart-Phillips, 1986). SIMULPS14 will solve simultaneously for variations in *Vp* and in *Vp/Vs* ratio. It was found, however, that the present data set contained insufficient S-wave arrival data and only P-wave velocities were inverted for. Using the same constant value for the *Vp/Vs* ratio as before, *Vs* values were derived from the P model at each node so that S-wave arrivals could be used in the relocation stage. Station corrections were also used in the relocation stage but damped so that they remained unchanged during the inversion.

As can be seen in Figure 3, the ray-path coverage of Scotland is very variable and it is desirable to maximise the resolution in areas with most data while avoiding over-interpretation of sparse data in other regions. A graded inversion strategy (Eberhart-Phillips, 1990) was used to best utilise the flexible gridding capabilities of SIMULPS14. A first pass was carried out with node spacing of 40km. Then, the derivative weight sum (DWS) (Thurber and Eberhart-Phillips, 1999) was used to decide

which parts of the grid were sufficiently well resolved. After some experimentation a value of 32 was used as the threshold. A second pass was then executed with node spacing of 20km but with those nodes at or between less well resolved 40km nodes fixed to the values from the previous run. The results here thus represent 20 km grid spacing but with some neighbouring nodes set to the same value as each other – the value they had at the end of an inversion at 40 km grid spacing. The improvement in total rms using the 20km model rather than the 40km model is 0.01 seconds. The greatest velocity changes between the two models are of the order of 4%.

Resolution of the resulting model was estimated using a chequerboard test (Humphreys and Clayton, 1988). A synthetic model with 40km node spacing was created divided into alternating regions of velocity 5% higher and lower than that in the minimum 1-D model. This model was used to generate replacement travel times for the events using ray tracing. The arrival times were then perturbed randomly by up to 0.05 seconds to mimic picking uncertainty and used with the original hypocentres as input for a standard SIMULPS run with the starting model of interest. The results are shown in (Figure 8). Those parts of the 3-D model where the synthetic velocities were recovered were considered to correspond to parts of the actual output model that are well resolved. Unsurprisingly, these are the same parts of the model as those that the most ray-paths traverse, as revealed by examining the DWS for different nodes. The shallowest part of the model is not well resolved by the available data except in the central part of the model, where the number of stations in relatively high. At greater depths, the model is generally well resolved, with the best resolution in the mid-Crust. This suggests that the data coverage is sufficient to resolve features with a scale length of at least 40 km and above. Model resolution is noticeably poorer at most depths in the east part of the model and towards the north coast.

To confirm the interpretation of the chequerboard test three other resolution tests were carried out. Figure 9 shows the results of these for one depth only so that they can be compared with each other and with the chequerboard test. In the first instance the DWS itself is plotted, in the second the diagonal element of the resolution matrix is shown. The spread function is a measure of resolution that is less dependent on grid spacing and damping than simply looking at the diagonal element (Reyners et al., 1999). This is shown in the third panel of Figure 9. All of these measures of resolution can be seen to confirm the choice to limit the finer inversion grid to the region shown in the forth panel, which shows those nodes allowed to change in the second inversion.

3-D modes were calculated using the tomographic inversion scheme for the nine best 1-D models determined by VELEST (Figure 6). In each case the 1-D model was transformed into a simulps starting model by placing nodes at the layer boundaries with velocities equal to the average of the layers above and below the boundary. The final model was chosen by the quality of the chequerboard test (Figure 8) and the accuracy with which quarry events (Figure 5) were relocated, as well as by the final variances in data and model parameters. The simulps starting model based on VELEST model 2 is the starting model that produced the best 3-D tomographic model, this model is shown in Figure 6. It is the 3-D model obtained using this starting model that is discussed below.

Results

The final model of P-wave velocity is shown in Figure 10. As explained above, this is computed on a 20 km grid, although, in some areas the resolution is less than this. This model incorporates the station corrections output by VELEST (Figure 7) and these remain unchanged in the solution. In general, the model shows relatively little lateral variation in seismic velocity at each depth and velocities remain similar to the 1-D starting model. This suggests that when velocities are averaged over a 20-40km grid the differences across Scotland are rather small, despite the observed variation in surface geology.

The uppermost layer is poorly constrained by the data, with insufficient rays passing near the surface to get a velocity at all for several nodes near the centre of the country. In addition, the upper layer needs to be looked at in conjunction with the station corrections (figure 7) as smaller scale changes will be accounted for here, rather than in the velocity model. Despite this, there is good correlation between the low velocity zone in the centre of the model and the Midland Valley, a known sedimentary basin of Palaeozoic age. Immediately south of the Midland Valley, higher velocities are apparent across the Southern Uplands, particularly in the southwest part. These features are also clear at a greater depth of 3.5 km. The 3.5 km layer also shows slow velocities around the Moray Firth where at least 4km of Mesozoic sediment is present in basins (Trewin and Rollin, 2002) and between the Palaeogene lavas of Skye and Mull. There is a fast anomaly around Loch Ericht to the southeast of the Great Glen fault.

At depths of 7.5 and 10.5 km the model reveals fast velocity zones that appear to be associated with both the Proterozoic crystalline rocks of the Lewisian Complex, west of the Moine Thrust and also with the Paleogene lavas on Skye . Fast velocity regions in the model are also observed immediately north of the Highland Boundary Fault. At greater depths, model velocities are relatively uniform across all of Scotland, with the exception of the far northwest of Scotland and the Outer Hebrides, where they are faster. High velocities are also observed across northwest Scotland in the 30 km layer. This can be interpreted in terms of a Moho discontinuity that dips from northwest to southeast, with faster velocities to the northwest, where it is shallow and slower velocities in the Midland Valley where it is deep. A dipping Moho may also explain the bimodal appearance of the 1-D velocity model tests in Fig 4. Other anomalies outside these regions are artefacts resulting from the inversion.

Discussion

The Lithospheric Seismic Profile in Britain (LISPB) was an Anglo-German explosion seismic project shot in 1974 and designed to study the whole lithosphere below Britain (Bamford *et al.*, 1976). It included three segments of a line running north-south through Scotland and northern England. Eighteen shots of between two and six tons of explosive were recorded by up to 40 stations along this line. One of the products of this experiment was a 2-D velocity profile along the line (Bamford *et al.*, 1978), that has formed the basis of the velocity model used for earthquake location in Scotland ever since. (Barton, 1992) refined the 1978 LISPB model but her model remains broadly similar with the most obvious difference the addition of intermediate layers. This level of detail is not reached by the tomography discussed here and so it is reasonable to compare directly with the 1978 model for clarity. Figure 11 shows the location of the LISPB line and a copy of the line drawing by (Bamford *et al.*, 1978). A profile through the 3-D tomography model is shown for comparison. The profiles can be seen to be in general agreement with, for example the 6.5 kms^{-1} contour of the tomography model rising beneath the Midland Valley in the same way as the corresponding reflector in the 1978

profile. The depth of the Moho is difficult to distinguish in 3-D models like the one developed here. This is because it models the velocity gradient and the Moho is defined as a reflection from a discontinuity. The Moho appears to be represented in the new model by the contour at 7.5 kms^{-1}, which runs at a similar depth to the interface between 7.3 kms^{-1} and 8 kms^{-1} in the Bamford model.

A further active seismic experiment, the Midland Valley Investigation by Seismology (MAVIS), was carried out at right angles to the LISPB profile in 1984, looking at the upper crust along the Midland Valley (Dentith and Hall, 1989), (Conway *et al.*, 1987). Figure 12 shows a comparison between a line drawing of the results and a profile through the new 3-D model. Again there is general agreement, although the MAVIS results are much more detailed. The transition between velocities of 6.0 kms^{-1} and 6.5 kms^{-1} occurs in both cases at about 5 km with the faster zone becoming shallower as the profile is followed eastwards.

The Southern Uplands Seismic Profile (SUSP, (Hall *et al.*, 1983)) is oriented at right angles to LISPB, along the axis of the Southern Uplands. SUSP shows seismic velocities of 6.0 kms^{-1} at about 1 km depth increasing to 6.3 kms^{-1} by 4 km, significantly higher than those shown in the new model or the LISPB results. (Hall *et al.*, 1983) interpret these observations as a large-scale anisotropy in the structure of the Southern Uplands, with slices of high grade metamorphic or igneous rocks caught up between accretionary wedge sediments in a stack striking southwest northeast, parallel to SUSP.

Building on an earlier compilation by (Clegg and England, 2003), (Kelly *et al.*, 2007) combined data from a number of controlled source experiments, both onshore and offshore, to produce a 3-D seismic velocity model for the crust under the UK and surrounding area. Their results are difficult to compare to the new model, however, as the data available for their study was limited geographically. The average crustal velocity for the whole of the UK, Ireland and surrounding offshore areas is given as 6.14 kms^{-1} with a standard deviation of 0.34 by (Kelly *et al.*, 2007). This agrees well with the average velocity of the model presented here, which is 6.26 kms^{-1} in the area where all layers have defined velocities. A similar problem is found when comparing the new model with the Moho depth maps made by (Chadwick and Pharaoh, 1998). This study also used mainly offshore reflection and refraction data and the resulting resolution is very different to the resolution of the new model.

(Nicolson *et al.*, 2012) use ambient noise tomography to reveal velocity changes beneath Scotland north of the Highland Boundary Fault. They use surface waves in 3 frequency bands to image different depths. It is interesting to compare the relative group velocities from this method with the corresponding layers of the new model. The 5 second wavelength corresponds roughly to the model layer at 7.5 km and in both cases there is a east-west split in the velocity with velocities of the Lewisian Complex to the West being faster than those along the Great Glen Fault and to the east. There is no layer in the model to compare directly to the interferometry at wavelengths of 12 seconds. The 20 second wavelength compares to the model layer at 30 km – here the split is north-south and in both cases shows the Moho becoming shallower to the north as discussed above.

(Asencio *et al.*, 2003) used teleseismic receiver function techniques to study the upper mantle beneath a temporary array they installed near the north coast, just to the east of the LISPB profile. They concluded a crustal thickness of 24–26 km. Unfortunately the 7.5 kms^{-1} contour, which seems to best represent the Moho, is not mapped by the new model at this point (about 100km along the

LISPB profile in Figure 11). However, a few kilometres further along the profile the contour can be seen to be sloping upwards in a northerly direction at a depth of about 28km.

(Tomlinson, 2006), (Di Leo *et al.*, 2009) and (Davis *et al.*, 2012) all used teleseismic P-wave receiver functions to determine variations in crustal thickness and *Vp/Vs* ratio across Scotland. These studies essentially agree with the LISPB results and show crustal thickness varying from about 23 km in the north-eastern highlands to more than 30 km near the Highland Boundary Fault. These results also agree with the model found here.

There are two BIRPS (British Institutions Reflection Profiling Syndicate) deep seismic profiles that fall within the area modelled here. The WINCH (Hall *et al.*, 1984) profile runs along the whole west coast of Scotland to the west of the Hebrides. The NEC (Freeman *et al.*, 1988) profile runs just off the east coast between Montrose and Hartlepool. Both of these lines are too close to the periphery of the new model for a useful comparison to be made.

Improved location accuracy is another reason for calculating a better velocity model. One indication of this is the average of the root-mean-square residuals for the 405 events. Using the velocity model currently used at the BGS this average residual is 0.21 while the 3-D model results in an average residual of 0.13 (the average residual for the minimum 1-D model is 0.20). The change in location for earthquakes in the west of Scotland (359 of the 405 events used) is shown in Figure 13. The events are less scattered and in many areas lines of events are more clearly seen. In other studies these lines of relocated earthquakes delineating faults show dipping planes but this is not the case here. This may be because the faults in the west of Scotland dip very steeply, as suggested in (Baptie, 2010). Deeper events are mostly relocated to shallower depths.

To test the accuracy of locations made with the new 3-D model the quarry blasts used to discriminate between the 1-D models (Figure 5) were again used. Relocation of the quarry events using SIMULPS14 with the 1-D starting model resulted in the events being relocated, on average just over 5km from the quarries they originated from. This was worse than the relocation done with VELEST using the same model, presumably because the layer model had been transformed to gradients for use with simulps. When the same events were relocated using the new 3-D model the blasts were, on average, within 4km of the relevant quarry. Location errors were however, not uniformly distributed between the quarries. The quarries at the edge of the new model, where it is acknowledged to be less accurate, had much larger errors than those within the area of the models' highest resolution and in some cases (the quarry on Orkney, for example) the new model made the relocation worse than before. It was decided to relocate only those quarry blasts from the Glensanda quarry in the north-west highlands. These account for about half of the quarry events being used (26 blasts) and the quarry is located in the centre of the new model where coverage is best. As Figure 14 shows, these locations are markedly more accurate when calculated using the new model than with the 1-D model – the average distance from the quarry has fallen from 5359m to 3278m.

Conclusions

A 3-D velocity model has been developed for Scotland using local earthquake tomography. This model has varying resolution at different depths in different areas. The best resolution at all depths is in the west of the country and through the Midland Valley. Resolution is poorer at most depths in

the east and towards the north coast. Where the model is well resolved it agrees well with the published results of reflection and refraction experiments in and around Scotland and with previous tomography and receiver function studies. However, the models show relatively little lateral variation in seismic velocity except at shallow depths, where sedimentary basins such as the Midland Valley are apparent. At greater depths, higher velocities in the northwest parts of the models suggest that the thickness of crust increases towards the south and east. This observation is also in agreement with previous studies. The model is suitable for earthquake location and, as a result of the method used, is best resolved where it will be most needed for this. Relocation of quarry blasts and earthquakes indicate that significantly better solutions for earthquakes in the seismically active part of Scotland will result from the use of this new model.

Acknowledgements

The authors thank Ilaria Mosca and Maarten Krabbendam for useful comments on the manuscript and Richard England, Jun Korenaga and an anonymous reviewer for a helpful review of the paper. This work is published with the permission of the Executive Director of the British Geological Survey (NERC).

References

Aki, K., Christoffersson, A. & Husebye, E.S., 1977. Determination of 3-Dimensional Seismic Structure of Lithosphere, *J. Geophys. Res.,* 82**,** 277-296.

Arrowsmith, S.J., Kendall, M., White, N., VanDecar, J.C. & Booth, D.C., 2005. Seismic imaging of a hot upwelling beneath the British Isles, *Geology,* 33**,** 345-348.

Asencio, E., Knapp, J.H., Owens, T.J. & Helffrich, G., 2003. Mapping fine-scale heterogeneities within the continental mantle lithosphere beneath Scotland: Combining active- and passive-source seismology, *Geology,* 31**,** 477-480.

Bamford, D., Faber, S., Jacob, B., Kaminski, W., Nunn, K., Prodehl, C., Fuchs, K., King, R. & Willmore, P., 1976. A Lithospheric Seismic Profile in Britain—I Preliminary Results, *Geophys. J. Roy. Astron. Soc.,* 44**,** 145-160.

Bamford, D., Nunn, K., Prodehl, C. & Jacob, B., 1978. LISPB – IV. Crustal structure of Northern Britain, *Geophys. J. Roy. Astron. Soc.,* 54**,** 43-60.

Baptie, B. ,2010. Seismogenesis and state of stress in the UK, *Tectonophysics,* 482**,** 150-159.

Barton, P.J., 1992. LISPB revisited: a new look under the Caledonides of northern Britain, *Geophys. J. Int.,* 110**,** 371-391.

Bastow, I.D., Owens, T.J., Helffrich, G. & Knapp, J.H., 2007. Spatial and temporal constraints on sources of seismic anisotropy: Evidence from the Scottish highlands, *Geophys. Res. Lett.,* 34.

Booth, D.C., J., B.J.D. & M., O.M.A., 2001. The UK seismic velocity model for earthquake location - a baseline review : British Geological Survey Report IR/01/188, pp. 18.

Bott, M.H. & Bott, J.D., 2004. The Cenozoic uplift and earthquake belt of mainland Britain as a response to an underlying hot, low-density upper mantle, *Journal of the Geological Society,* 161**,** 19-29.

Bott, M.H.P., Long, R.E., Green, A.S.P., Lewis, A.H.J., Sinha, M.C. & Stevenson, D.L., 1985. Crustal structure south of the Iapetus suture beneath northern England, *Nature,* 314**,** 724-727.

Chadwick, R.A. & Pharaoh, T.C., 1998. The seismic reflection Moho beneath the United Kingdom and adjacent areas, *Tectonophysics,* 299**,** 255-279.

Clegg, B. & England, R., 2003. Velocity structure of the UK continental shelf from a compilation of wide-angle and refraction data, *Geological Magazine,* 140**,** 453-467.

Conway, A., Dentith, M.C., Doody, J.J. & Hall, J., 1987. Preliminary interpretation of upper crustal structure across the Midland Valley of Scotland from two East–West seismic refraction profiles, *Journal of the Geological Society,* 144**,** 865-870.

Coward, M.P., 1983. The thrust and shear zones of the Moine thrust zone and the NW Scottish Caledonides, *Journal of the Geological Society,* 140**,** 795-811.

Davis, M.W., White, N.J., Priestley, K.F., Baptie, B.J. & Tilmann, F.J., 2012. Crustal structure of the British Isles and its epeirogenic consequences, *Geophys. J. Int.,* 190**,** 705-725.

Dentith, M.C. & Hall, J., 1989. Mavis - an Upper Crustal Seismic Refraction Experiment in the Midland Valley of Scotland, *Geophys. J. Int.,* 99**,** 627-643.

Di Leo, J., Bastow, I.D. & Helffrich, G., 2009. Nature of the Moho beneath the Scottish Highlands from a receiver function perspective, *Tectonophysics,* 479**,** 214-222.

Eberhart-Phillips, D., 1986. Three-dimensional velocity structure in northern California Coast Ranges from inversion of local earthquake arrival times, *Bull. Seismol. Soc. Am.,* 76**,** 1025-1052.

Eberhart-Phillips, D., 1990. Three-Dimensional P and S Velocity Structure in the Coalinga Region, California, *J. Geophys. Res.,* 95**,** 15343-15363.

Edwards, J. & Blundell, D., 1984. Summary of seismic refraction experiments in the English Channel, Celtic Sea and St. George's Channel, *Rep. Br. geol. Surv. MGRP,* 144.

Evans, J., Eberhart-Phillips, D. & Thurber, C.H., 1994. User's manual for SIMULPS 12 for imaging Vp and Vp/Vs: A derivative of the "Thurber" tomographic inversion SIMUL3 for local earthquakes and explosions, *U.S. Geol. Surv. Open-File Rept.,* 94-431**,** 101.

Freeman, B., Klemperer, S.L. & Hobbs, R.W., 1988. The deep structure of northern England and the Iapetus Suture zone from BIRPS deep seismic reflection profiles, *Journal of the Geological Society,* 145**,** 727-740.

Hall, J., Brewer, J.A., Matthews, D.H. & Warner, M.R., 1984. Crustal structure across the Caledonides from the 'WINCH' seismic reflection profile: influences on the evolution of the Midland Valley of Scotland, *Earth and Environmental Science Transactions of the Royal Society of Edinburgh,* 75**,** 97-109.

Hall, J., Powell, D.W., Warner, M.R., El-Isa, Z.H.M., Adesanya, O. & Bluck, B.J., 1983. Seismological evidence for shallow crystalline basement in the Southern Uplands of Scotland, *Nature,* 305**,** 418-420.

Hardwick, A., 2008. New insights Into the crustal structure of the England, Wales and Irish Seas areas from local earthquake tomography and associated seismological studies, Ph.D., University of Leicester.

Haslinger, F. & Kissling, E., 2001. Investigating effects of 3-D ray tracing methods in local earthquake tomography, *Phys. Earth Planet. In.,* 123**,** 103-114.

Humphreys, E. & Clayton, R.W., 1988. Adaptation of Back Projection Tomography to Seismic Travel Time Problems, *J. Geophys. Res.,* 93**,** 1073-1085.

Husen, S., Kissling, E., Deichmann, N., Wiemer, S., Giardini, D. & Baer, M., 2003. Probabilistic earthquake location in complex three-dimensional velocity models: Application to Switzerland, *J. Geophys. Res.,* 108.

Jacob, A.W.B., Kaminski, W., Murphy, T., Phillips, W.E.A. & Prodehl, C., 1985. A crustal model for a northeast-southwest profile through Ireland, *Tectonophysics,* 113**,** 75-103.

Kelly, A., England, R.W. & Maguire, P.K.H., 2007. A crustal seismic velocity model for the UK, Ireland and surrounding seas, *Geophys. J. Int.,* 171**,** 1172-1184.

Kissling, E., 1988. Geotomography with local earthquake data, *Rev. Geophys.,* 26**,** 659-698.

Kissling, E., 1995. Velest Users Guide, *Internal report, Institute of Geophysics, ETH, Zurich*.

Kissling, E., Ellsworth, W.L., Eberhart-Phillips, D. & Kradolfer, U., 1994. Initial reference models in local earthquake tomography, *J. Geophys. Res.,* 99**,** 19635-19646.

Kissling, E., Husen, S. & Haslinger, F., 2001. Model parameterization in seismic tomography: a choice of consequence for the solution quality, *Phys. Earth Planet. In.,* 123.

Kissling, E., Solarino, S. & Cattaneo, M., 1995. Improved seismic velocity reference model from local earthquake data in Northwestern Italy, *Terra Nova,* 7**,** 528-534.

Klemperer, S. & Hobbs, R., 1992. *The BIRPS Atlas: Deep Seismic Reflections Profiles Around the British Isles*, Cambridge University Press.

Maguire, P., England, R. & Hardwick, A., 2011. LISPB DELTA, a lithospheric seismic profile in Britain: analysis and interpretation of the Wales and southern England section, *Journal of the Geological Society,* 168**,** 61-82.

Main, I., Irving, D., Musson, R. & Reading, A., 1999. Constraints on the frequency–magnitude relation and maximum magnitudes in the UK from observed seismicity and glacio-isostatic recovery rates, *Geophys. J. Int.,* 137**,** 535-550.

Nicolson, H., Curtis, A., Baptie, B. & Galetti, E., 2012. Seismic interferometry and ambient noise tomography in the British Isles, *Proceedings of the Geologists' Association,* 123**,** 74-86.

Pavlis, G.L. & Booker, J.R., 1980. The mixed discrete-continuous inverse problem: Application to the simultaneous determination of earthquake hypocenters and velocity structure, *J. Geophys. Res.,* 85**,** 4801-4810.

Reyners, M., Eberhart-Philipps, D., Stuart, G., 1999. A three-dimensional image of shallow subduction: crustal structure of the Raukumara Peninsula, New Zealand, *Geophys. J. Int*., 137, 873-890

Simpson, B.A., 2007. Bulletin of British Earthquakes 2006, *British Geological Survey Internal Report,* OR/07/003.

Spencer, C. & Gubbins, D., 1980. Travel-time inversion for simultaneous earthquake location and velocity structure determination in laterally varying media, *Geophys. J. Roy. Astron. Soc.,* 63**,** 95-116.

Stone, P. & Smellie, J.L., 1988. *Classical areas of British geology: the Ballantrae area. Description of the solid geology of parts of 1:25 000 sheets NX 08, 18 and 19,* edn, Vol., pp. Pages, H.M.S.O., London.

Strachan, R.A., 2000. The Grampian Orogeny: Mid-Ordovician arc-continent collision along the Laurentian margin of Iapetus. *in Geological History of Britain and Ireland*, eds. Woodcock, N. & Strachan, R. A. Wiley - Blackwell.

Thurber, C.H., 1983. Earthquake Locations and Three-Dimensional Crustal Structure in the Coyote Lake Area, Central California, *J. Geophys. Res.,* 88**,** 8226-8236.

Thurber, C.H. & Eberhart-Phillips, D., 1999. Local earthquake tomography with flexible gridding, *Comput. Geosci.,* 25**,** 809-818.

Tomlinson, J.P., P. Denton P. K. H. Maguire D. C. Booth, 2006. Analysis of the crustal velocity structure of the British Isles using teleseismic receiver functions, *Geophys. J. Int.,* 167**,** 223-237.

Trewin, N.H. & Rollin, K.E., 2002. Chapter 1: Geological history and structure of Scotland. *in The Geology of Scotland*, ed. Trewin, N. H. Geological Society.

Woodcock, N. & Strachan, R.A., 2000. The Caledonian Oregeny: a multiple plate collision. *in Geological History of Britain and Ireland*, eds. Woodcock, N. & Strachan, R. A. Wiley - Blackwell.

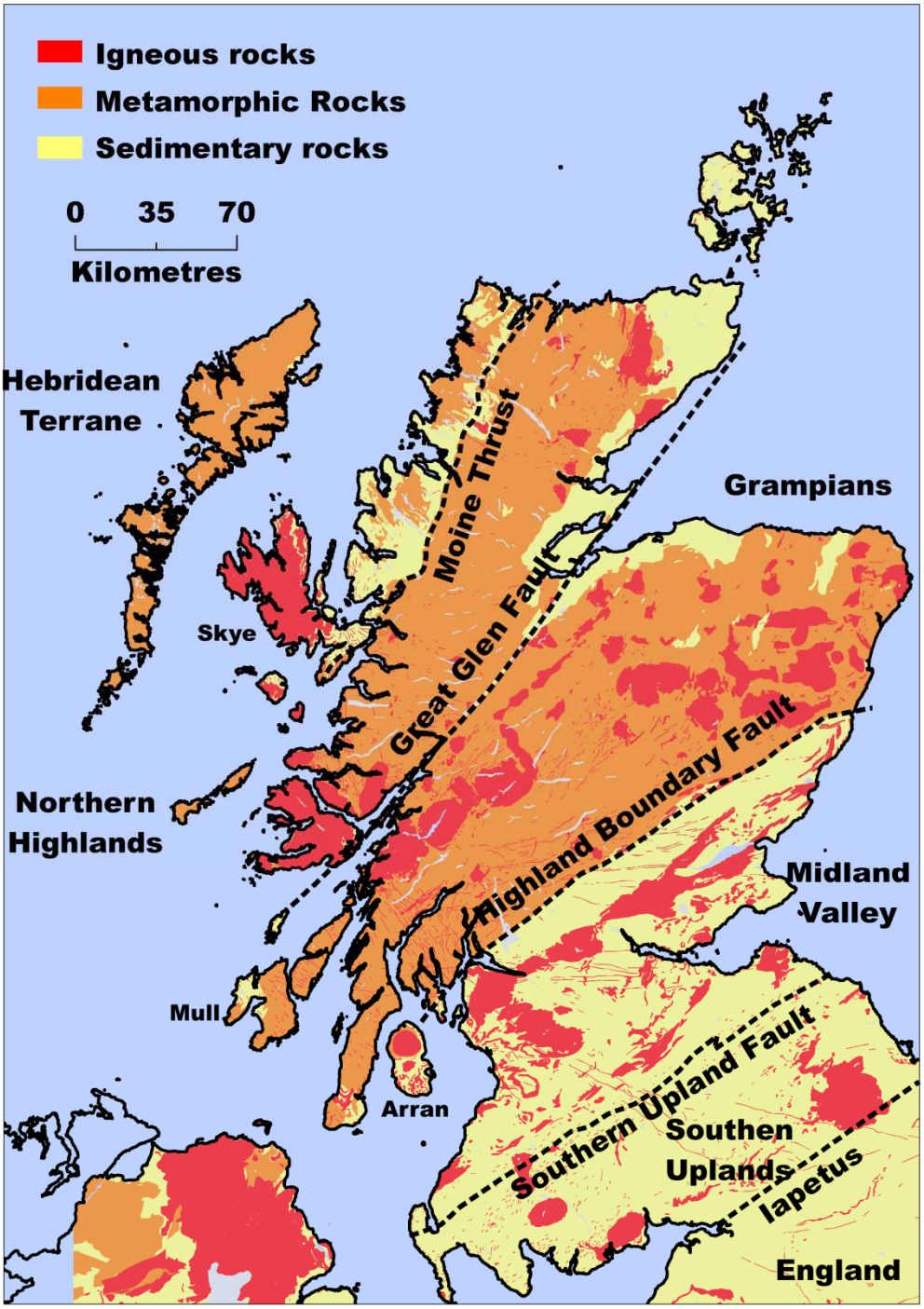

Figure 1: Surface geology of Scotland. The major faults are shown which separate the different terranes discussed in the text.

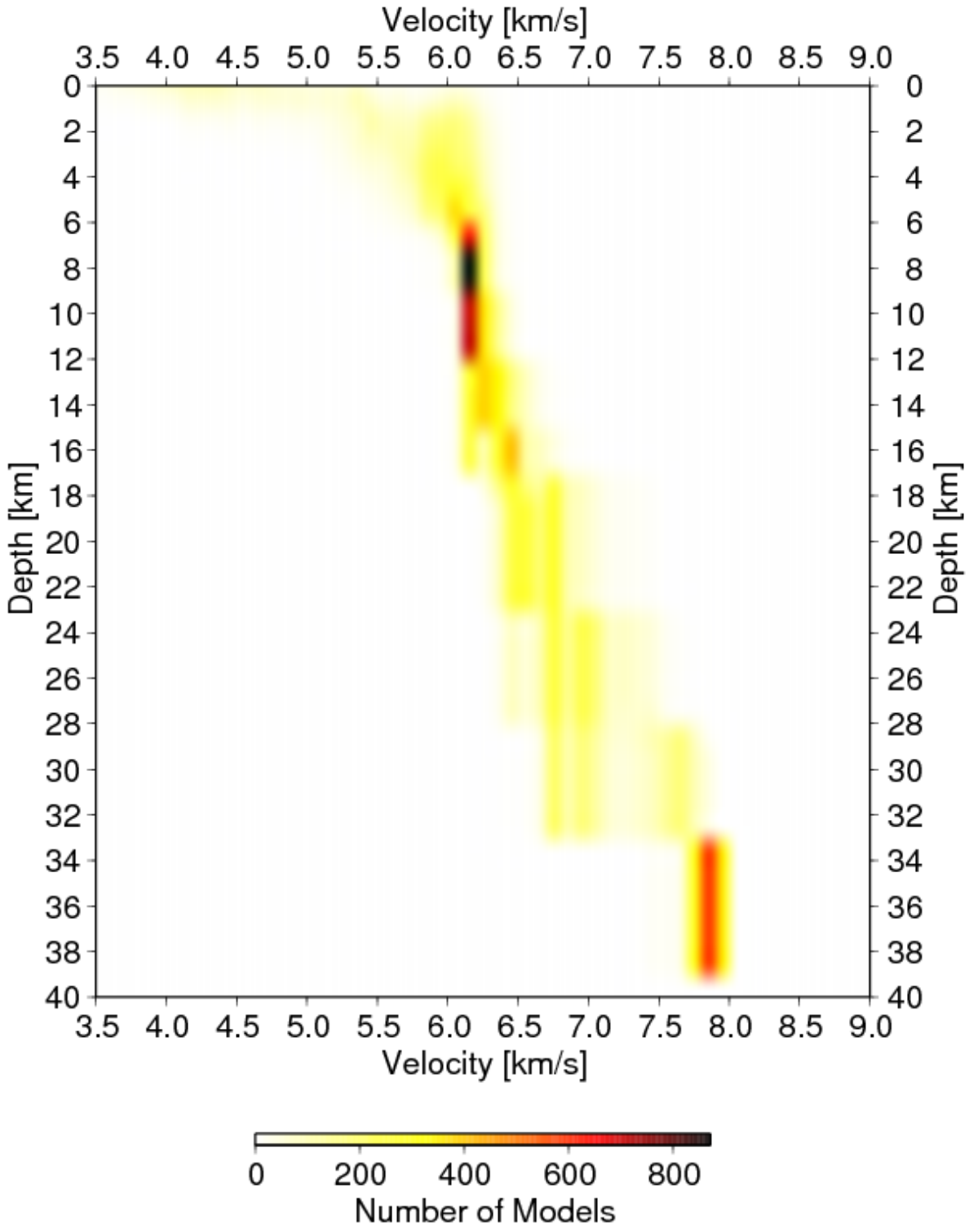

Figure 4: The 1200 1-D models found using VELEST for 1200 different starting models selected randomly using 4 different layer structures. The number of resulting models is contoured over cells of 0.1 ms^{-2} in velocity and 1 km in depth.

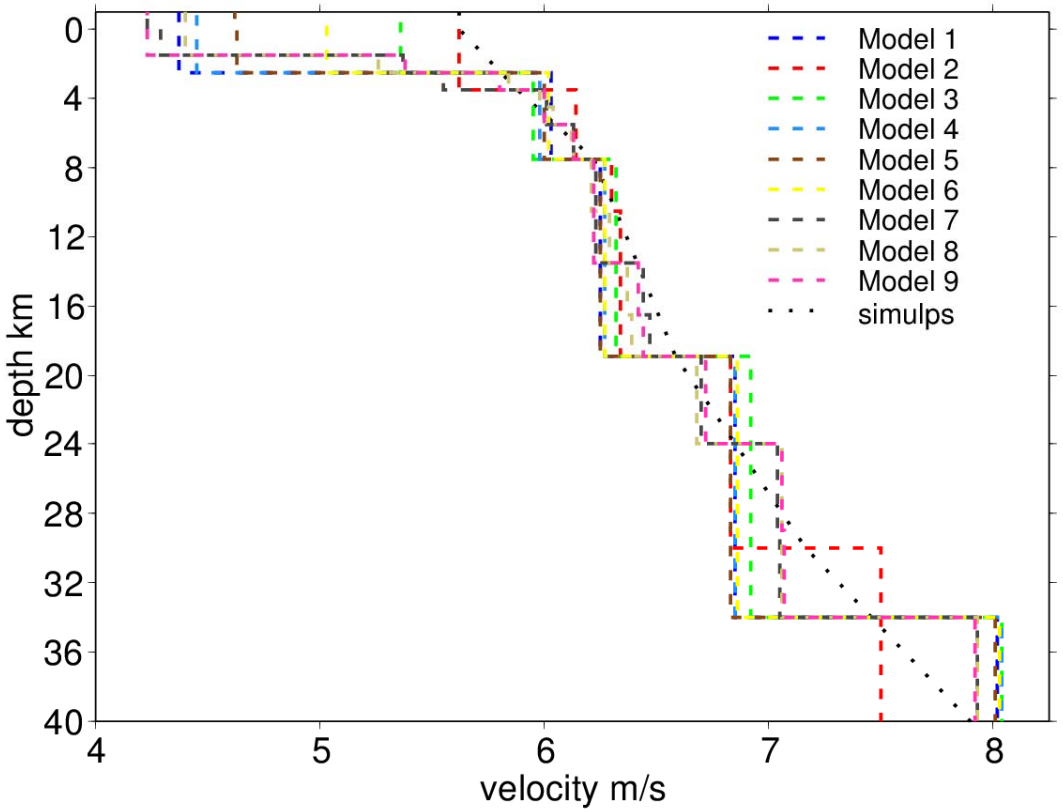

Figure 6: The 9 best 1-D models found for the dataset using VELEST and the gradational model used as the input model for simulps.

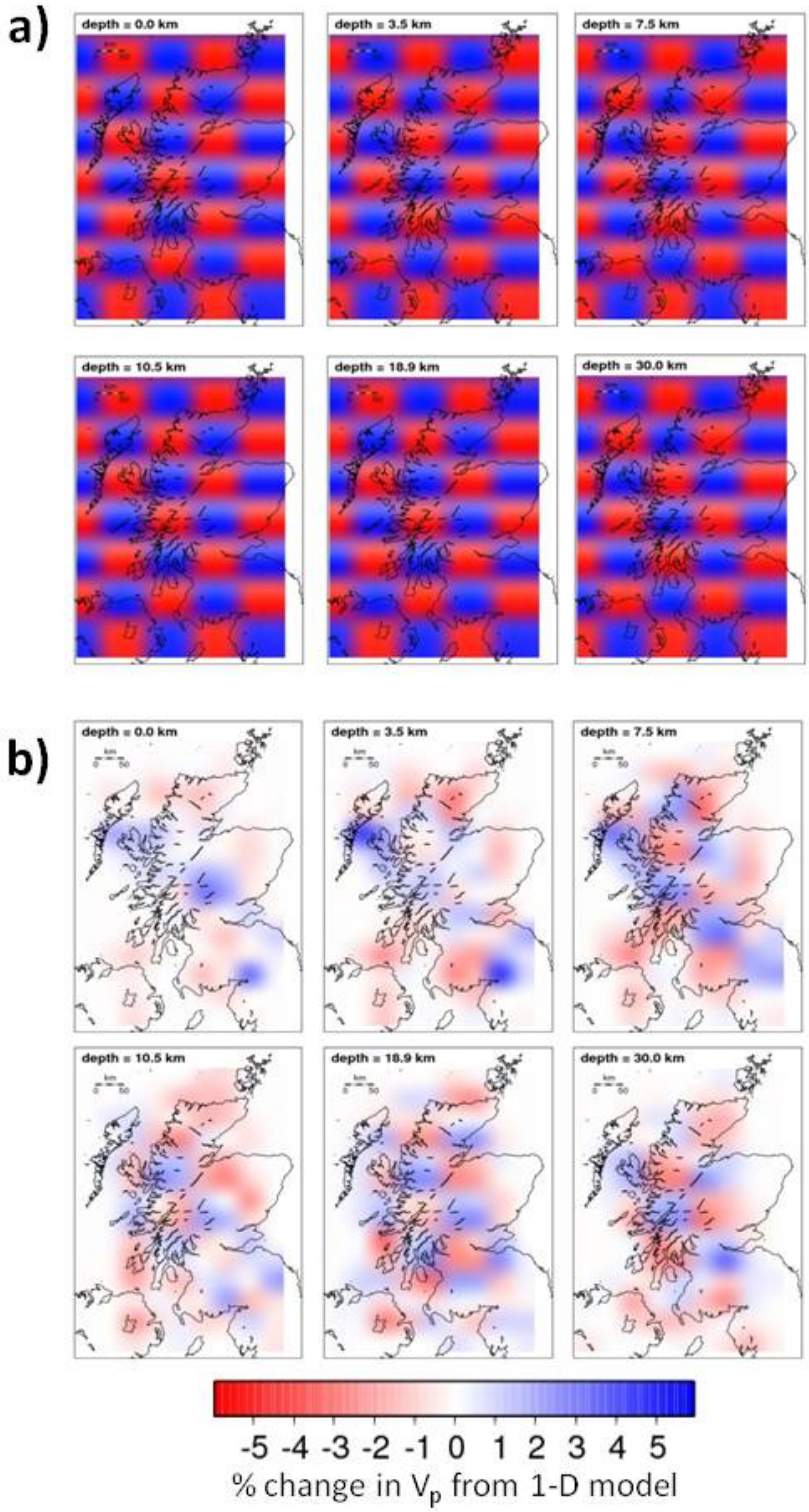

Figure 8: Results of chequerboard test for the final model. a) Is the synthetic model used to generate travel times and b) is the model found when using these travel times, slightly perturbed, as input.

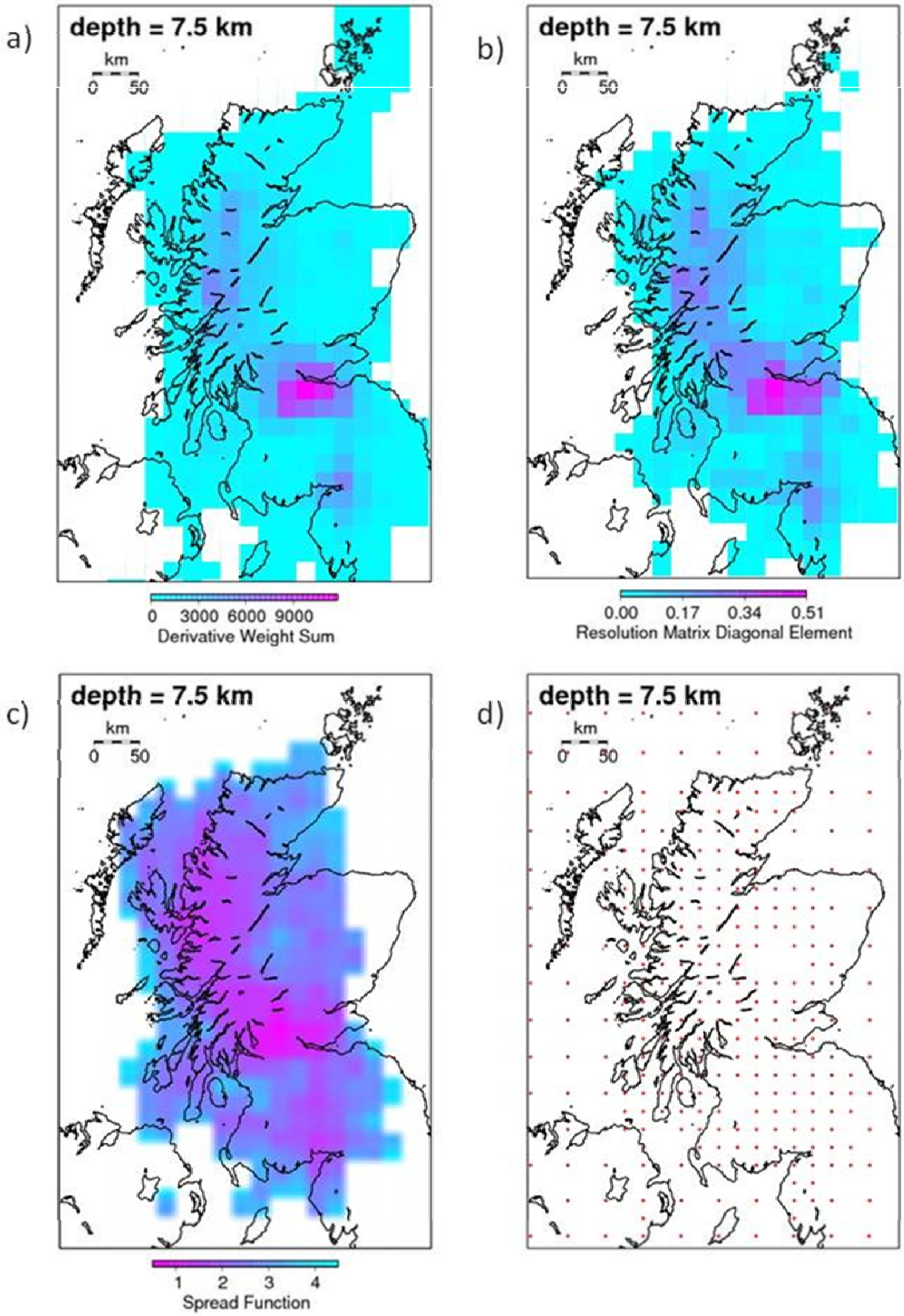

Figure 9: Three measures of resolution for the final velocity model at a depth of 7.5 km. a) The derivative weight sum (DWS). b) The resolution matrix diagonal element (RDE). c) The spread function. In d) the nodes that were allowed to change in the final inversion are plotted. This shows where the node spacing was 20km and where it remained at 40km, as in the first inversion.

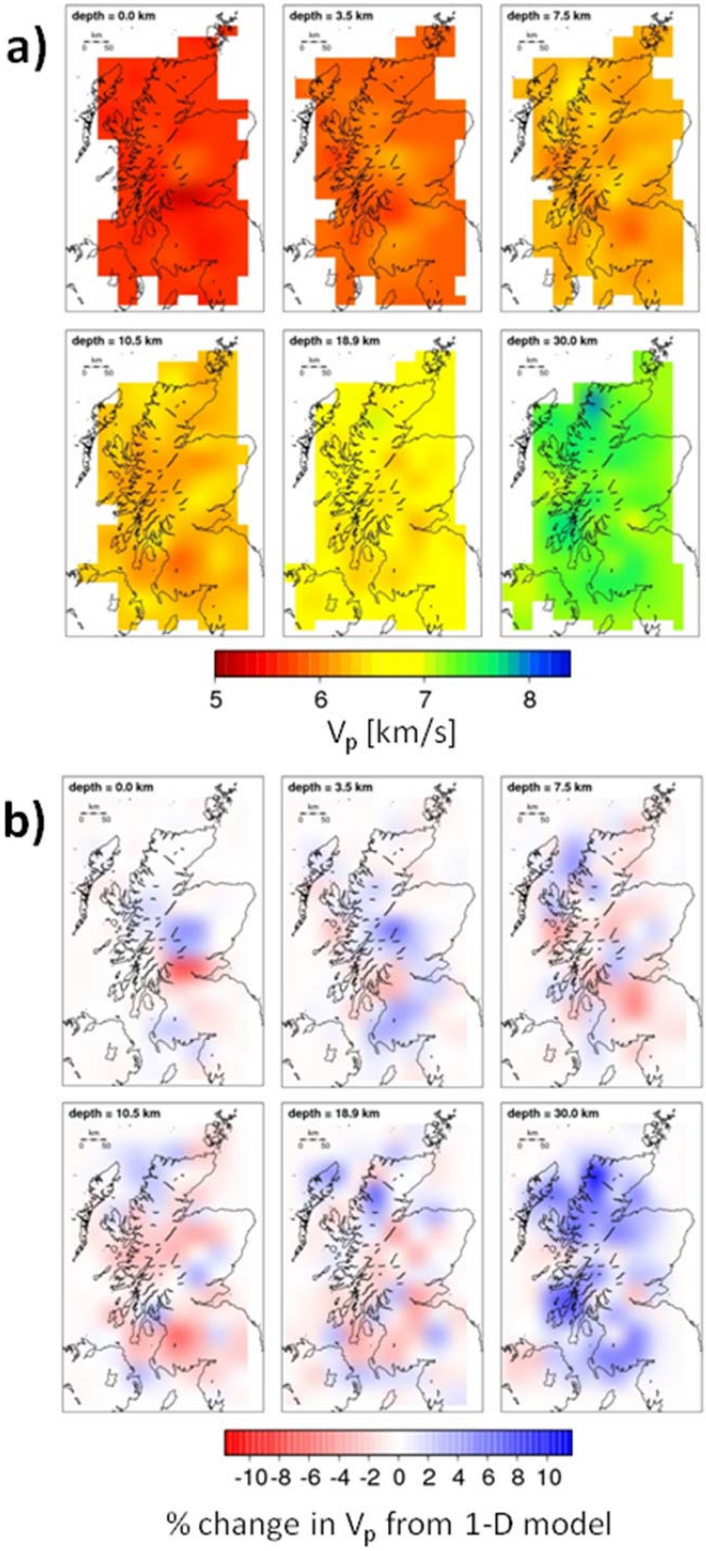

Figure 10: Results from local earthquake tomography for Scotland using SIMULPS14 for data from 405 earthquakes. a) Shows absolute velocity with the same scale for all layers. b) Shows the same data but displayed as % perturbation from the starting model.

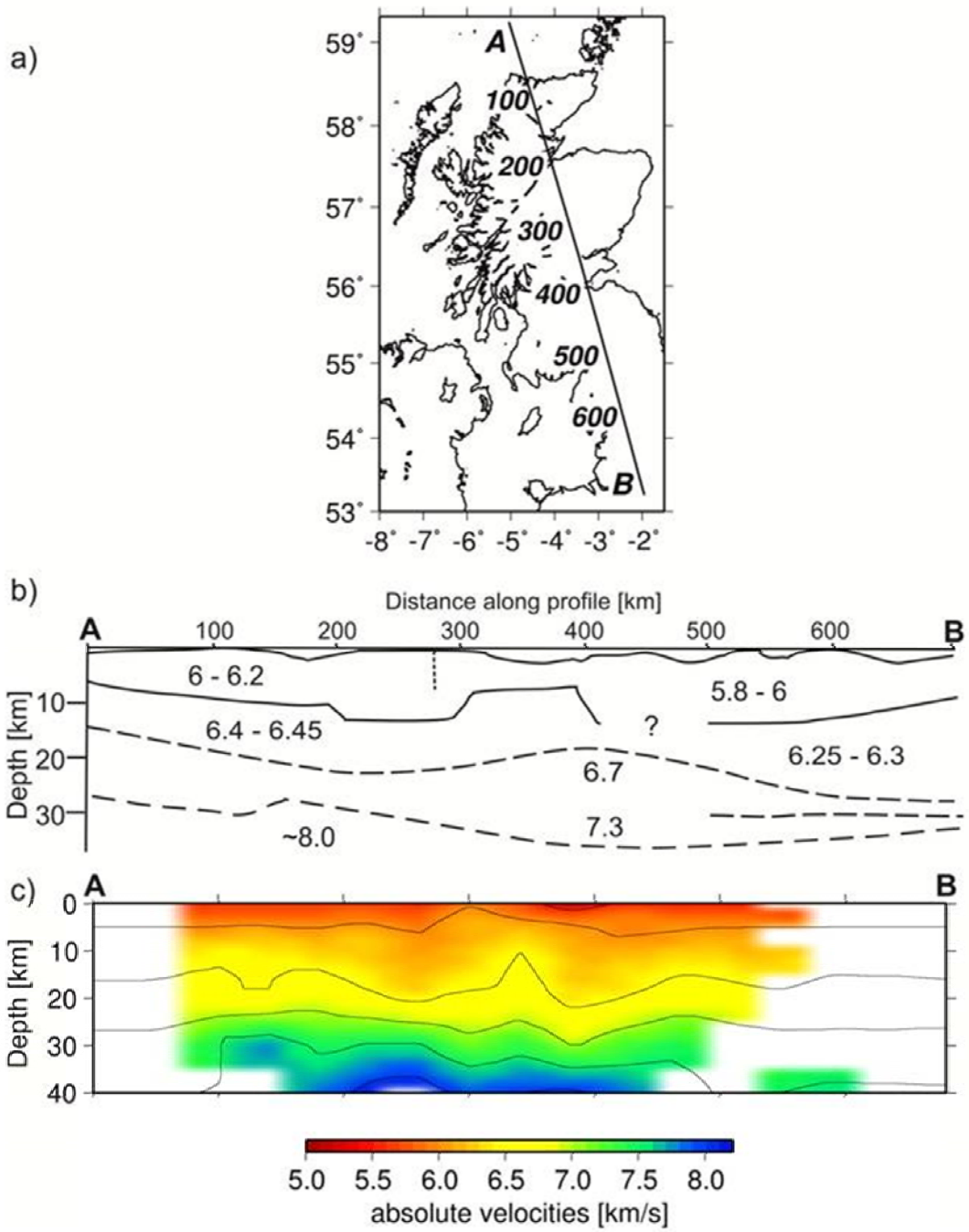

Figure 11: Comparison between the results of the LISPB experiment and the new tomographic model.

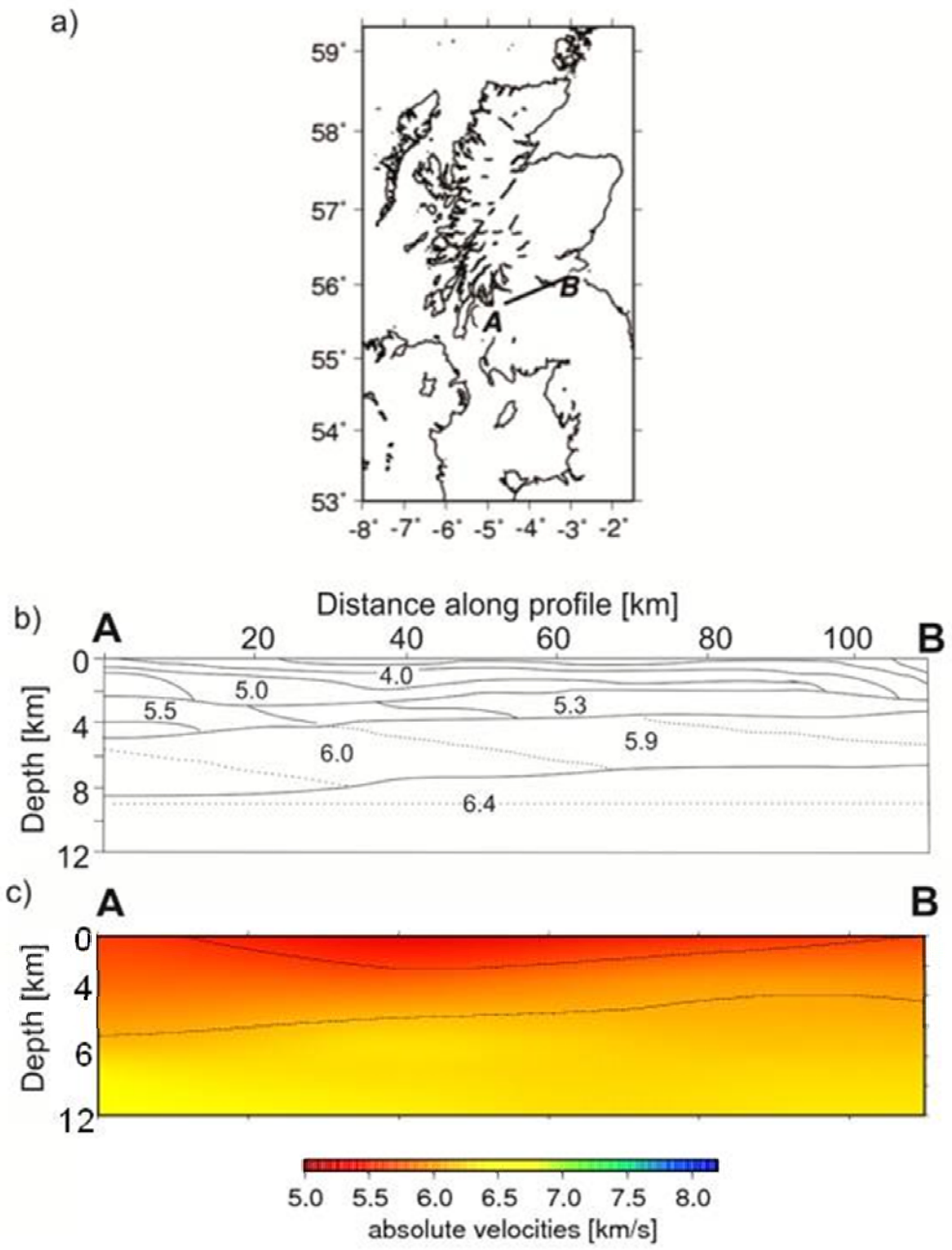

Figure 12: Comparison between the MAVIS seismic experiment and the new tomographic model.

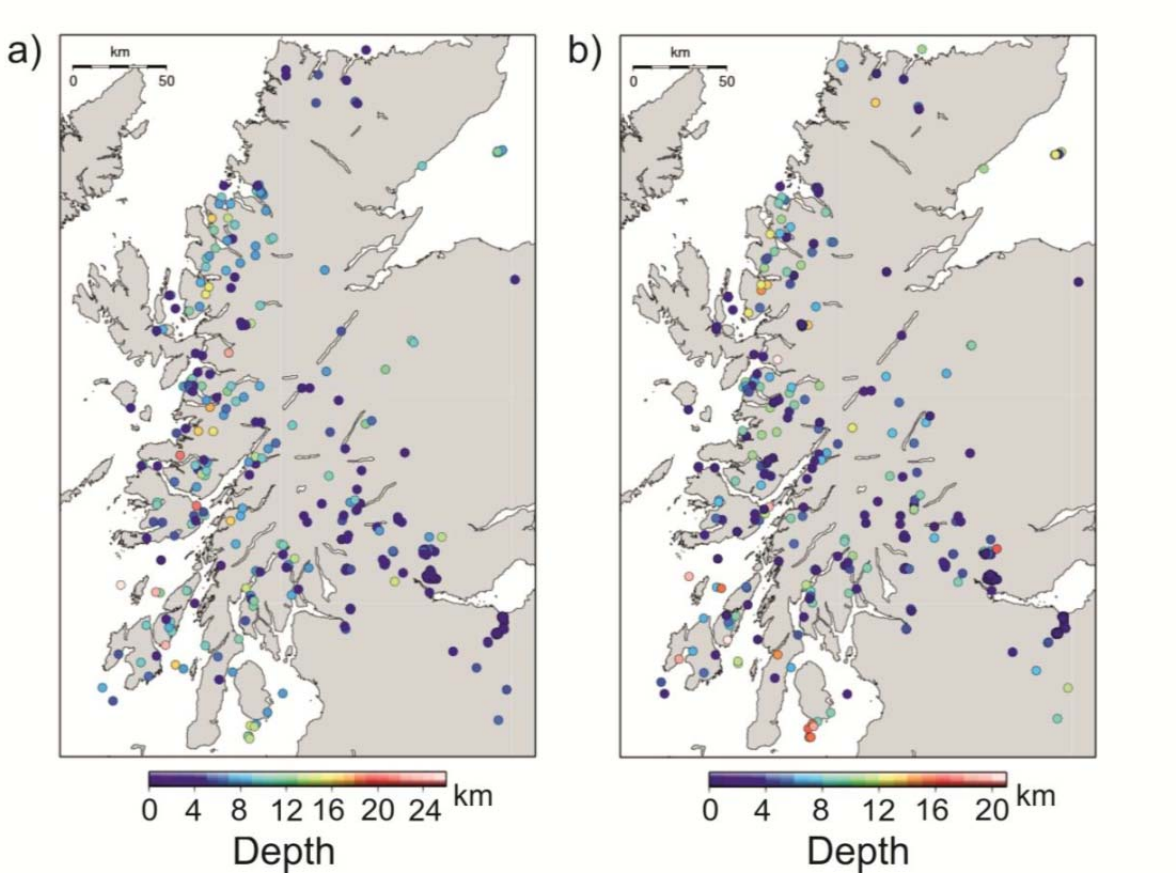

Figure 13: Epicentres for earthquakes in the study region a) locations using the existing 1-D velocity model, b) locations using the new 3-D model. Note the bunching of earthquakes into tighter groups in the second map.